Supporting Information

Kinetic-Dynamic Model for Conformational Control of an Electron Transfer Photocycle: Mixed-Metal Hemoglobin Hybrids

Ami D. Patel, Judith M. Nocek, Brian M. Hoffman*

These equations are taken from Ref 6, but recast in the notation used in this paper

$$T(t) = a_1 e^{-ft} + b_1 e^{-gt} \qquad \textbf{Eq 10a}$$

$$I(t) = c_1 e^{-ft} + c_2 e^{-gt} + c_3 e^{-mt} + c_4 e^{-nt} \qquad \textbf{Eq 10b}$$

$$(f,g) = \tfrac{1}{2}[2k_D + k_d + k_u + k_t^R + k_t^S \mp \sqrt{(k_u + k_d)^2 + (k_t^R - k_t^S)(k_t^R - k_t^S + 2k_d - 2k_u\}}] \qquad \textbf{Eq S1}$$

$$a_1 = \frac{k_x - f}{g - f},$$

$$a_2 = \frac{g - k_x}{g - f}$$

$$k_x = k_D + k_u + k_d + F^R k_t^R + F^S k_t^S$$

$$(m,n) = \tfrac{1}{2}[k_b^R + k_b^S + k_{dI} + k_{uI} \mp \sqrt{(k_{dI} + k_{uI})^2 + (k_b^R - k_b^S)(k_b^R - k_b^S + 2k_{dI} - 2k_{uI})}] \qquad \textbf{Eq S2}$$

$$c_1 = \frac{af^2 + bf + c}{(g - f)(m - f)(n - f)},$$

$$c_2 = \frac{ag^2 + bg + c}{(f - g)(m - g)(n - g)},$$

$$c_3 = \frac{am^2 + bm + c}{(f - m)(g - m)(n - m)},$$

$$c_4 = \frac{an^2 + bn + c}{(f - n)(g - n)(m - n)}$$

$$a = k_t^S + (k_t^R - k_t^S)F^S$$

$$-b = k_t^R[k_u + F^S(k_{uI} + k_{dI} + k_b^S + k_t^S + k_D) + k_t^S[k_d + F^R(k_{uI} + k_{dI} + k_b^R + k_t^R + k_D)]$$

$$c = k_t^R(k_{uI} + k_{dI} + k_b^S)[k_u + F^S(k_t^S + k_D)] + k_t^S(k_{uI} + k_{dI} + k_b^R)[k_d + F^R(k_t^R + k_D)]$$

Yields and Detectibility

The solutions to the kinetic equations (**Eqs 3-10**) of the KD model give the progress curves for **T** and **I**, and these can be decomposed into the fractional contributions of various ET 'routes'. The contribution of a route to a measured signal, however depends both on the kinetic yield of the route, and on 'detectability' factors defined here.

Forward ET Yields: The fractional yield of forward ET that occurs within the T^S and T^R conformations is $\phi^i = (k_t^i F^i)/k_{obs}$, where i = S or R, the fractional occupancies (F^i) are defined in **Eq 12**, and the appropriate k_{obs} is specific to the limit/regime under consideration; **Table S1** gives the yields for the three limits/regimes discussed explicitly. **Table S1** further decomposes the fraction of ET occurring from the T^R conformation into two contributions: *i*) the fraction that occurs with ET rate constant k_t^R, denoted ϕ^R, and *ii*)the fraction that originates in T^S and represents gated ET that occurs with conformational rate constant k_u (denoted ϕ^G)

We note that the yields in the *SE* limit are simply given by the equilibrium populations, [F^S, F^R], when [k_t^R, k_t^S] >> k_D, but when this inequality does not hold the yields can differ substantially, and this is the case for the experiments of this paper.

Back ET Yields: In both the *FE* and *SE* limits the total yield of back ET from I^S and I^R would be given by the equilibrium populations, [F^S, F^R], if [k_t^R, k_t^S] >> k_D. In the antigating regime or when in *SE* limit [k_t^R, k_t^S] is not much greater than k_D, the yield of ET occurring through I^S and I^R will be equivalent to the amount of forward ET occurring through T^S and T^R respectively.

Detectability of Contributions to T: In principle, the triplet decay would be biphasic under any conditions except the *FE* limit, with decay constants that are combinations of ET and conformational rate constants, and thus can vary with viscosity. However it is difficult to experimentally detect the more rapidly decaying contribution to the progress curve when $K^S >> 1$. In such cases the contribution of T^R (fraction F^R) is small enough to not be reliably detected by experiment, and as a result the triplet decay in general is effectively mono-exponential throughout the entire dynamic range from *FE* to *SE*, with an observed forward ET rate constant that depends upon conformational dynamics. In short, one would expect just the kind of variation in the triplet-decay constant with viscosity seen for the hybrids (**Fig 5**).

Detectability of Contributions to I: Unlike the timecourse of **T**, the contribution of each phase to the observed absorbance change for **I** is not simply governed by its kinetic yield determined from the microscopic rate constants. The maximum amplitude (P_{max}) of the phase, which we denote the 'detectability because it corresponds to its maximum absorbance, can be written as the product of two factors. The first is the yield for that phase (ϕ) as discussed above; the second is the fraction of that yield that actually accumulates at the time of maximum amplitude. This 'accumulation factor (δ)' is a function of the ratio of the rate constants for the appearance and disappearance of that phase, k_p and k_b of **Eq 2**, and has two different forms depending on which of the two rate constants is greater. When $k_b > k_p$ ('rapid disappearance'),

$$P^{rap}_{max} = \phi \cdot \delta^{rap}, \qquad \delta^{rap} = n^{-(n/(n-1))} \quad n \equiv k_b/k_p > 1 \qquad \textbf{Eq S3}$$

whereas when $k_b < k_p$ ('slow disappearance'),

$$P^{slo}_{max} = \phi \cdot \delta^{slo}, \qquad \delta^{slo} = m^{-(1/(m-1))} \quad m \equiv k_p/k_b > 1 \qquad \textbf{Eq S4}$$

Most of the routes that contribute to the timecourses for the hybrids are of the former type ($n > 1$), in which case their accumulation factors suppress their contributions to the overall decay, $\delta^{rap} < 1$. If a system exhibits both slowly-disappearing and rapidly disappearing phases, the different forms of the accumulation factors guarantee that the signal for the slowly-disappearing phase almost always will dominate the observed timecourse, even if the yield of the rapidly-disappearing phase is greater.

Table S1

Route	ϕ^i, Forward ET		
	S	R	
		From T^R	Gated
FE	$F^S(k_t^S/k_{obs}^{eq})$	$F^R(k_t^R/k_{obs}^{eq})$	--
SE	$F^S(k_t^S/k_{obs}^S)$	$F^R(k_t^R/k_{obs}^R)$	
G/A	--	$F^R(k_t^R/k_{obs}^R)$	$F^S(k_u/k_{obs})$

Table S2: ET yield of individual triplet species at low, intermediate, and high viscosity.

		T^S	T^R
ϕ_{ET}	*FE*	0.068	0.23
	SE	0.088	0.029
	η = 15 cP	0.084	0.078

Table S3: Detectability of kinetic routes at low, intermediate and high viscosity.

	Routes					
	FE	*SE*		η = 15 cP		
	-	*S*	*R*	*S*	*R*	*G/A*
ϕ^i	0.296	0.0881	0.0285	0.0835	0.0285	0.0501
ϕ^i_{rel}	100	76	24	51	18	31
ϕ_{TOTAL}	0.296	0.117		0.162		
n	2.96	3.63	1.03	3.45	1.03	10.38
δ	0.194	0.168	0.373	0.175	0.373	0.0751
P_{max}	0.0575	0.0148	0.0106	0.0146	0.0106	0.00376
$[P_{max}]_{rel}$	1.0	1.0	0.72	1.0	0.73	0.23

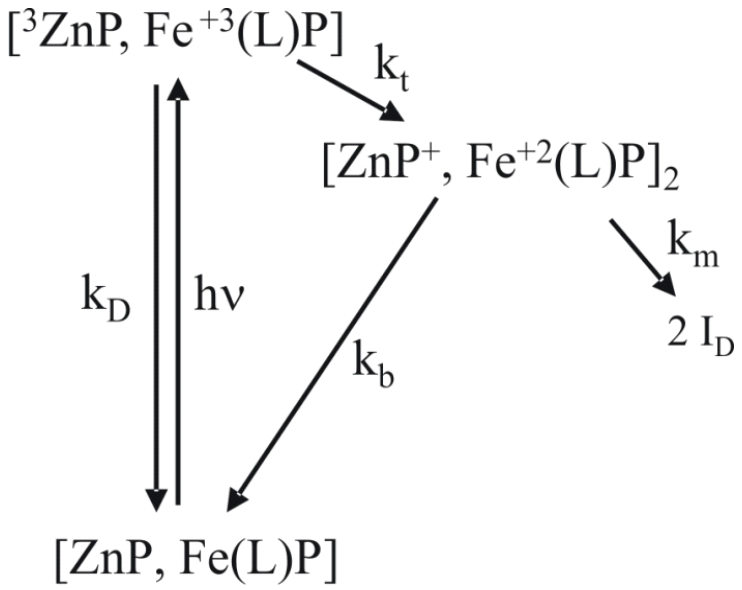

Scheme S1

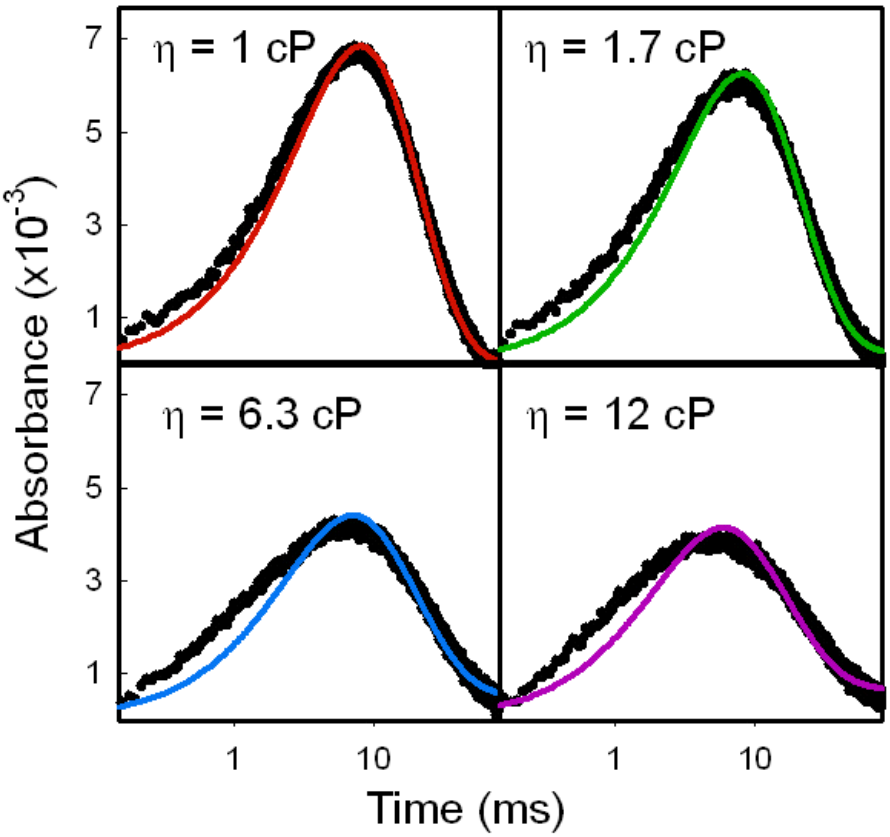

S1: Experimental **I** timecourses (black) at η = 1, 1.7, 6.3, and 12 cP overlaid with fits to **Eq 2** with $k_p = k_{obs}$.

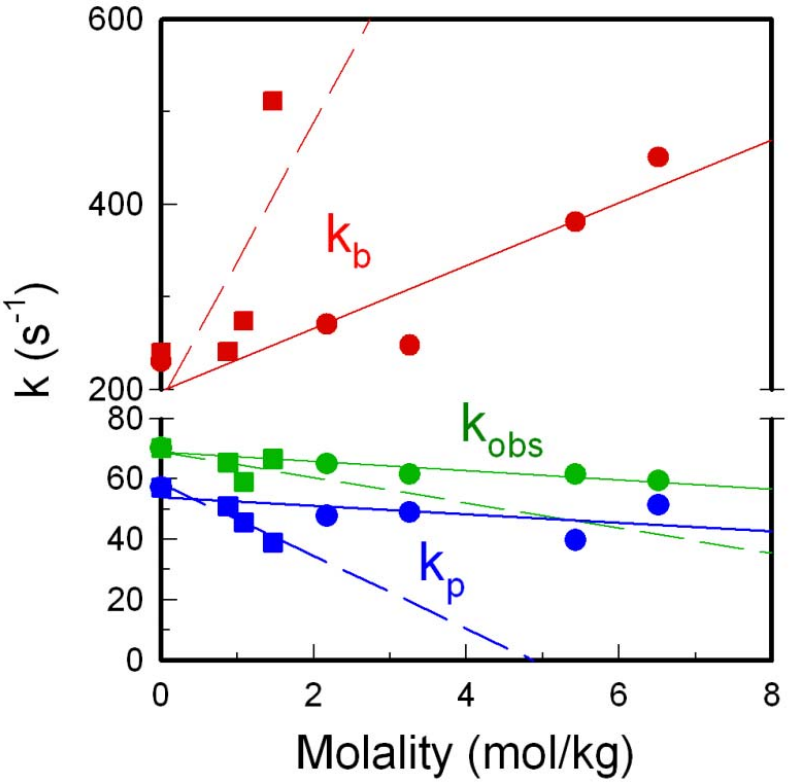

S2: ET rate constants, k_b (red), k_p (blue), and k_{obs} (green) as a function of sucrose (■) or glycerol (●) molality: k_{obs} from fits of **T** to **Eq 1**; k_b and k_p from fits of timecourse for **I** to **Eq 2** ($k_p \neq k_{obs}$ permitted). Dashed and solid lines are fits of sucrose or glycerol data, respectively, to a linear regression curve.

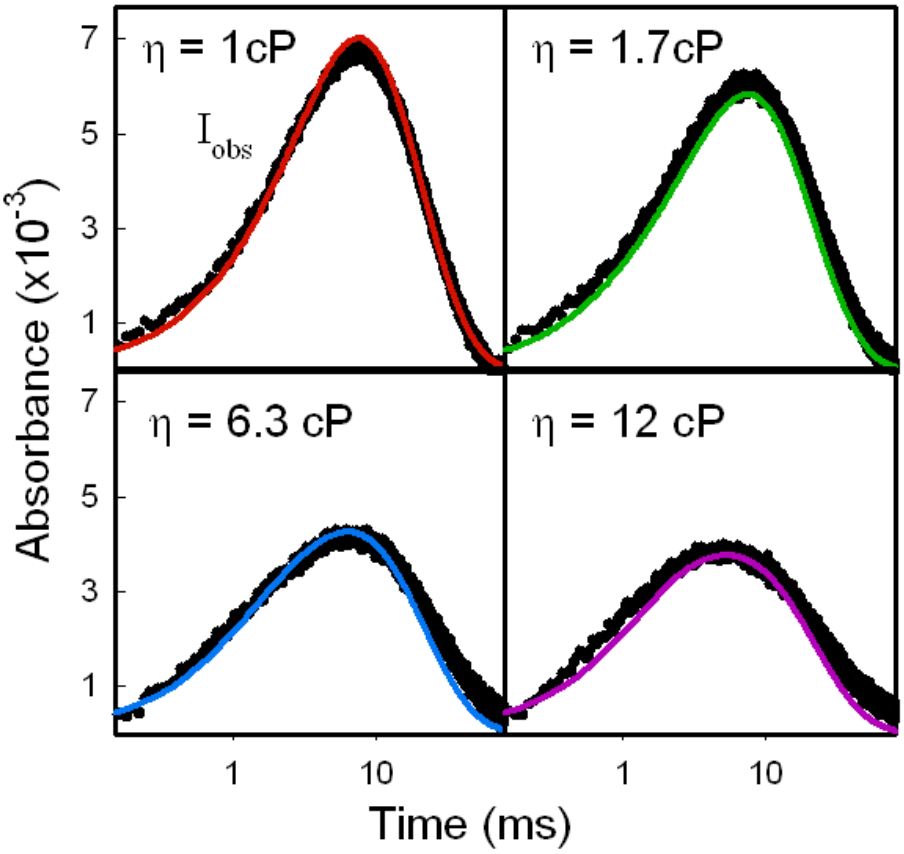

S3: Experimental **I** timecourses (black) at η = 1, 1.7, 6.3, and 12 cP overlaid with simulated KD traces calculated with initial parameters in **Table 1**.